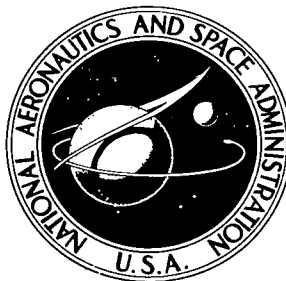


NASA TECHNICAL NOTE



NASA TN D-4595

2.1

NASA TN D-4595



LOAN COPY: RETURN TO  
AFWL (WLIL-2)  
KIRTLAND AFB, N MEX

# ANALYTICAL INVESTIGATION OF ELECTRICALLY HEATED WIRE MESH FOR FLOWING GAS HEATERS

*by William F. Mattson and William L. Maag*

*Lewis Research Center*

*Cleveland, Ohio*



NATIONAL AERONAUTICS AND SPACE ADMINISTRATION • WASHINGTON, D. C. • JUNE 1968

TECH LIBRARY KAFB, NM



0100740

ANALYTICAL INVESTIGATION OF ELECTRICALLY HEATED WIRE MESH  
FOR FLOWING GAS HEATERS

By William F. Mattson and William L. Maag

APPENDIX B: COMPUTER PROGRAM

By Geraldine E. Amling

Lewis Research Center  
Cleveland, Ohio

NATIONAL AERONAUTICS AND SPACE ADMINISTRATION

---

For sale by the Clearinghouse for Federal Scientific and Technical Information  
Springfield, Virginia 22151 - CFSTI price \$3.00

## ABSTRACT

An analytical method is presented whereby an electrical resistance, flowing gas heater can be designed using wire mesh as the heating elements. By specifying the gas, the flow rate, the system pressure, the desired inlet and outlet gas temperatures, and the power supply characteristics, a compatible wire mesh heater element design can be determined. The calculations involve solving simultaneous equations for the heat generation rate, the convective heat transfer from the mesh to the gas, and the change in enthalpy of the gas at every axial position along the heater length. The method also enables the determination of the operating conditions of an existing mesh heater when used at some off-design condition or with another gas.

STAR Category 12

# ANALYTICAL INVESTIGATION OF ELECTRICALLY HEATED WIRE MESH FOR FLOWING GAS HEATERS

by William F. Mattson and William L. Maag  
Lewis Research Center

## SUMMARY

An analytical method is presented whereby an electrical resistance flowing gas heater can be designed using wire mesh as the heating elements. By specifying the gas, the flow rate, the system pressure, the desired inlet and outlet gas temperatures, and the power supply characteristics, a compatible wire mesh heating element design can be determined. The calculations involve solving simultaneous equations for the heat generation rate, the convective heat transfer from the mesh to the gas, and the change in enthalpy of the gas at every axial position along the heater length. By varying the wire diameter, pitch, and size of the wire mesh, the designer is able to match the heater conditions to practically any type of power supply. The analytical method permits optimizing the heater design for compactness for specified operating conditions and limiting conditions such as maximum surface temperature or heat flux. It also enables one to determine the operating conditions of an existing mesh heater when used at an off-design condition or with another gas.

## INTRODUCTION

High temperature, out-of-pile tests of nuclear fuel elements have been conducted at the Lewis Research Center using hot flowing gas to simulate reactor operating conditions. Electrical resistance heaters were developed to heat the flowing gas. One type of heater consisted of electrically heated wire mesh through which the gas flows. The analytical investigation leading to the design of the wire mesh heating elements is the subject of this report.

The specific requirement was to design a heater utilizing an existing power supply to heat hydrogen, helium, and nitrogen gases at specified flow rates to temperatures up to 2780° K. The search for a suitable heating element led to a commercially available tungsten wire mesh made of helical coils. The mesh provided the capability of obtaining

electrical resistance compatible with the current and voltage ratings of available power supplies and also possessed a large surface area for heat transfer. Tungsten with its high melting point was chosen because of the high gas temperature requirement. A literature survey revealed only a limited amount of low temperature experimental heat transfer data for wire mesh. References 1 and 2 report the results of a Lewis experimental program to establish high temperature forced convection heat transfer correlations for electrically heated wire mesh.

After a heat transfer correlation was established, the task of using the mesh to design a heater capable of delivering gas at the desired flow rate and temperature remained. This involved solving simultaneous equations for the heat generation rate, the convective heat transfer from the mesh to the gas, and the change in enthalpy of the gas at every axial position along the heater length. This report investigates the variables in mesh geometry that can be utilized to achieve compact heater designs for limiting conditions such as maximum mesh surface temperature or heat flux. It defines reasonable limits within which a mesh heating element can be expected to operate satisfactorily. Two power supplies representing high and low electrical resistances are considered to illustrate how a mesh can be adapted to each. Experimental data from an operating mesh heater are presented to corroborate the analytical results.

A computer program by Geraldine E. Amling is included as appendix B.

## METHOD OF ANALYSIS

In designing an electrical resistance gas heater certain operating conditions must be specified. These include the type of gas, the gas flow rate and pressure, the initial and final gas temperature, and the current and voltage rating of the power supply. The next step then is to design a heating element that can generate and transfer heat to the flowing gas at a reasonable heat flux and at a surface temperature that would ensure a reasonable heater life. For this investigation, two different power supplies are considered. One represents a high resistance system in which the current can be maintained between 150 and 1500 amperes at voltages up to 3750 volts. The second represents a low resistance system whereby the voltage can be controlled between 10 and 50 volts at currents up to 60 000 amperes. The working gas is hydrogen at a flow rate of 0.0453 kilogram per second with an inlet temperature of  $278^{\circ}$  K and a desired outlet temperature of  $2780^{\circ}$  K.

### Mesh Heating Element

Tungsten wire mesh that can be electrically heated to surface temperatures greater

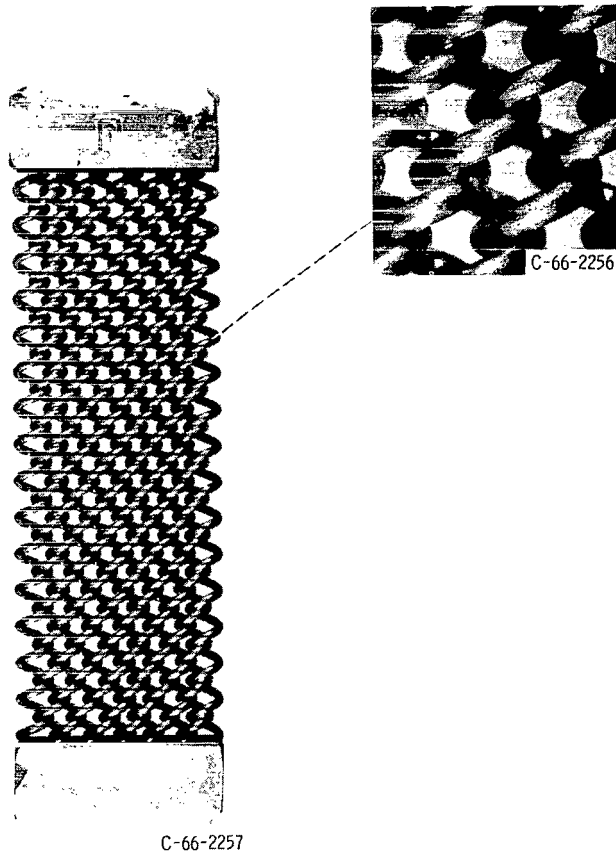


Figure 1. - Mesh heating element.

than 2780<sup>0</sup> K becomes a unique heater element when a nonelectrically conductive fluid flows through it. The mesh provides a large heat transfer surface area per unit volume of heater element that results in high power densities and small compact heaters. The 7.6- by 2.5- by 0.36-centimeter mesh shown in figure 1 has a surface area to volume ratio of 19 (cm<sup>2</sup>/cm<sup>3</sup>). The surface area of this mesh is equivalent to that of a 2.54-centimeter-diameter tube, 16.3 centimeters long. The chief disadvantage of a mesh element, as with any porous media, is the pressure drop restriction it places on fluid flowing through it. If relatively high pressure drops can be tolerated, then wire mesh provides many of the features necessary in a good heater element.

The wire mesh heater element considered herein is represented by figure 1. The element consists of helical coils of tungsten wire interwound into a mesh. Both ends of the coils are sandwiched between two tungsten plates each 0.153 centimeter thick. The plates and the coil ends are heliarc welded together at both ends of the mesh. The plates provide electrical bus connections for directing current through the coils. The total cur-

rent to the end plates will distribute itself into each wire coil according to the resistance of that coil. If the coolant flow distribution is uniform throughout the mesh, then the heat flux will be uniform and each coil will carry an equal amount of current. This is a necessary assumption for the analysis made herein although experimental results indicate that such is not always true. Reference 2 states that interwound mesh heating elements are susceptible to hot spotting and subsequent burnout at conditions of high heat flux with a nondissociating gas such as helium. This is believed to be caused by slight nonuniformities in the interwound geometry resulting in flow maldistribution within the mesh. If the mesh heat flux is maintained below some predetermined critical value, then the previous assumption is correct.

In order to calculate the heat transfer from a mesh it is necessary to know such geometrical parameters as surface area, current cross-sectional area, current path length, porosity, and equivalent diameter. These will be defined in terms of wire diameter, inside coil diameter (commonly referred to as mandrel diameter), coil pitch, number of parallel coils per width of mesh, and mesh length. The length  $S$  of wire in a single helical coil is given in reference 3 as

$$S = \frac{b}{p} \sqrt{\pi^2(D + d)^2 + p^2} \quad (1)$$

where  $b$  is the mesh length between end plates,  $p$  is the coil pitch,  $D$  is the inside coil diameter, and  $d$  is the wire diameter. (All symbols are defined in appendix A.) The total heat transfer surface area for  $N$  parallel coils is

$$A_s = \pi d S N \quad (2)$$

This was the area used in determining the heat transfer coefficients of references 1 and 2. The total current cross-sectional area for  $N$  parallel coils is

$$A_c = \frac{\pi d^2}{4} N \quad (3)$$

The average mesh porosity is defined as the ratio of void volume to total volume or

$$\epsilon = \frac{bw(D + 2d) - \frac{\pi d^2}{4} SN}{bw(D + 2d)} \quad (4)$$

where  $w$  is the mesh width and  $(D + 2d)$ , a coil diameter, represents the thickness in the flow direction. The equivalent diameter for a porous structure is usually defined as

$$D_e = \frac{4(\text{void volume})}{\text{surface area}} = \frac{4bw(D + 2d)\epsilon}{A_s} \quad (5)$$

The mass velocity of fluid through the element is based on an average flow area within the mesh as defined by the product of frontal area and porosity; that is,

$$G = \frac{W}{bwe} \quad (6)$$

For this analysis the mesh completely fills the flow passage so that there are no fluid by-pass effects as discussed in reference 1.

For this study, certain ground rules were established so that the mesh designs used were as compact as possible within reasonable limits for fabrication and assembly. For this reason the interwound helically coiled mesh of reference 1 was specified. The inside diameter of the coils was defined as  $2d + 0.005$  centimeter. The 0.005 centimeter allowed clearance for interwinding the coils. The coil pitch was defined as  $3d$  which represents the minimum allowable pitch for interwinding. The number of coils  $N$  can be expressed in terms of mesh width and the wire and mandrel diameters according to the following empirically derived equation:

$$N = 3 \left[ \frac{w - (2d + D)}{2d + D} \right] \quad (7)$$

This relation states that for a width  $w$ , less a half coil width on each side, the number of interwound parallel coils is three times the number that would be available if the coils were just placed side by side. Equation (7) is an approximation which is only to be used when coil pitch and mandrel diameter are defined as done previously. It is necessary that  $N$  always be evaluated as a whole number for any actual design.

With the foregoing set of rules different meshes having the same frontal dimensions were developed merely by changing the wire diameter, the other parameters all being defined in terms of this variable. Wire diameters from 0.036 to 0.127 centimeter were used for this study. A mesh made from wires smaller than 0.036 centimeter in diameter was considered from previous operating experience to be too flimsy, while a mesh made from wires having a diameter greater than 0.127 centimeter was considered too rigid for tungsten fabrication. The geometrical properties of representative meshes are given in table I for a 6.5-square-centimeter mesh (2.54 cm wide by 2.54 cm long). Prop-

TABLE I. - MESH GEOMETRY PARAMETERS

Wire diameter, d, cm	Mandrel diameter, D, cm	Number of parallel coils, N, coils/2.54 cm	Coil pitch, p, cm/turn	Mesh porosity, $\epsilon$	Ratio of total surface to frontal area, $A_s/A_f$ , $\text{cm}^2/\text{cm}^2$	Ratio of total wire length to current cross-sectional area, $S/A_c$ , $\text{cm}/\text{cm}^2$	Equivalent diameter, $D_e$ , cm
0.036	0.076	49	0.107	0.56	7.37	180	0.045
.051	.107	34	.152	.56	7.17	127	.066
.076	.157	22	.228	.58	6.84	87	.105
.102	.208	16	.304	.60	6.52	68	.151
.117	.239	13	.350	.61	6.34	60	.181
.127	.259	12	.381	.62	6.21	56	.204

erties such as surface area, equivalent diameter, and porosity relate to the heat transfer characteristics of the element while  $S/A_c$  is a measure of the electrical resistance.

### Mathematical Model

A physical model of two typical mesh stages is shown in figure 2. The gas enters

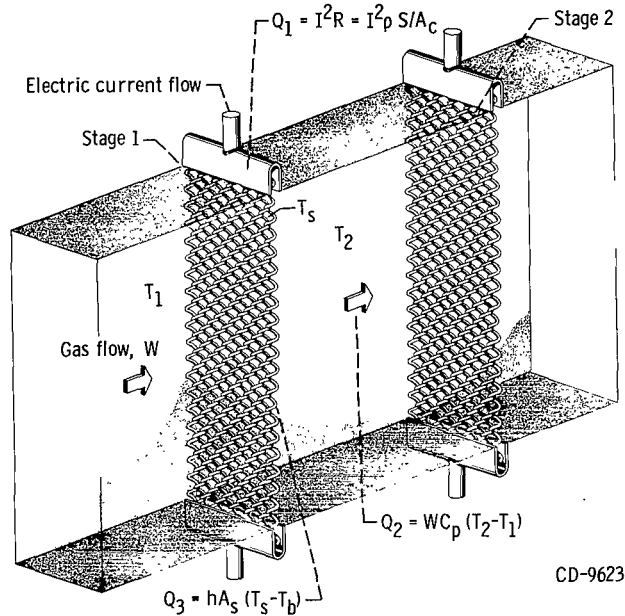


Figure 2. - Physical model.

upstream of stage 1 at temperature  $T_1$ . On passing through the electrically heated mesh of stage 1, heat is transferred to the gas by forced convection and exits at  $T_2$ ; that is,

$$Q = hA_s(T_s - T_b) \quad (8)$$

where

$$T_b = \frac{T_1 + T_2}{2} \quad (9)$$

The heat transfer coefficient  $h$  for interwound mesh was experimentally determined in reference 1 to be of the following form:

$$h = C \frac{k}{D_e} \left( \frac{GD_e}{\mu} \right)^n \left( \frac{C_p \mu}{k} \right)^{0.4} \quad (10)$$

Substituting equations (9) and (10) into equation (8) gives

$$Q = C \frac{k}{D_e} \left( \frac{GD_e}{\mu} \right)^n \left( \frac{C_p \mu}{k} \right)^{0.40} A_s \left( T_s - \frac{T_1 + T_2}{2} \right) \quad (11)$$

Viscosity  $\mu$  and thermal conductivity  $k$  values were obtained as functions of temperature and pressure from reference 4. Specific heat at constant pressure was evaluated at the stage inlet gas temperature using the specific heat-temperature correlation of reference 5. The electrical power input to the mesh heating element is given by the following equation in which either the voltage or current is specified depending upon the type of power supply available:

$$Q = \frac{V^2}{R} = I^2 R \quad (12)$$

where

$$R = \rho \frac{S}{A_c} \quad (13)$$

Resistivity  $\rho$  for most metals can usually be expressed as some function of temperature (ref. 6). Substituting equation (13) into equation (12) gives

$$Q = \frac{V^2}{\rho \frac{S}{A_c}} \quad (14)$$

The enthalpy rate increase of the gas is given by

$$Q = WC_p(T_2 - T_1) \quad (15)$$

The simultaneous solution of equations (11), (14), and (15) for a given set of conditions establishes the steady state heat transfer for the mesh-gas-power system. The three unknowns in these equations are the surface temperature  $T_s$ , the outlet gas temperature from stage 1  $T_2$ , and the rate of heat transfer  $Q$ . The numerical method of reference 7, chosen to solve these equations, was adapted to a digital computer. Appendix B presents details of the method as well as the computer program used. This analysis assumes an adiabatic system.

The computer program solves these equations for stage 1 and then proceeds to the next stage using the outlet gas temperature from stage 1 as the new inlet temperature. The calculations proceed stage by stage until the desired gas temperature is obtained or until certain predetermined limits such as surface temperature, heat flux, or number of stages are exceeded. When limits are reached, it is necessary to revise the mesh element design and repeat the calculations. The variables in mesh geometry that affect the calculations are discussed in the following section.

## RESULTS AND DISCUSSION

The most compact gas heater results when the heat transfer surface operates at a constant, maximum temperature. For a tube heater the equation

$$\frac{L}{D_t} = \frac{1}{2f} \ln \frac{T_w - T_{b1}}{T_w - T_{b2}} \quad (16)$$

gives the minimum length to diameter ratio for the case of constant wall temperature as derived by Reynold's analogy (ref. 8). For the design flow rates of this report, a tube

friction factor of 0.005 is reasonable. This results in an  $L/D_t$  of about 200. To electrically heat a tube of this length and maintain a constant wall temperature requires that the current cross-sectional area vary throughout the tube length. This is very difficult and impractical to do.

The advantages of a mesh heating element are compactness and design flexibility. The latter permits the designer to more or less specify the heat generation rate or the surface temperature at any axial position along the heater length. This may be accomplished by dividing the heater length into mesh stages in which the heat generation, heat transfer, and enthalpy for each stage or group of stages is specified. Then, by varying the mesh surface area, equivalent diameter, and ratio of current path length to cross-sectional area, it is possible to approximate the desired surface temperature or heat flux conditions. Referring to table I reveals that the surface area of the meshes investigated varied about 20 percent while the equivalent diameter and  $S/A_c$  varied by factors of 4.6 and 3.2, respectively.

Two design cases were investigated. One required a high electrical resistance mesh heater element, while the second required a low resistance element. Both cases specified hydrogen gas at 0.045-kilogram-per-second flow rate with an inlet temperature of  $278^{\circ}$  K and a desired outlet temperature of  $2780^{\circ}$  K. The system pressure was 100 atmospheres so that hydrogen dissociation was not a factor. The heater flow area was 25.8 square centimeters, and the mesh stage completely filled the flow passage cross-sectional area. The surface temperature of the mesh could not exceed  $3200^{\circ}$  K, and no more than 20 mesh stages were used. There was no limitation put on heat flux, but references 1 and 2 show that their maximum experimental value was about 1.24 kilowatts per square centimeter and the operating experience of reference 9 indicates that an average heat flux of 0.62 kilowatt per square centimeter seems reasonable for an extended period of operation. The heat transfer correlation of reference 1 was used for the calculations.

## High Voltage Heater Design

For a high voltage power supply the heater elements are connected electrically in series such that the same current flows in each mesh. The heat generated in each mesh stage is therefore proportional to the  $S/A_c$  ratio and the resistivity of tungsten at the temperature of the element. Figure 3 represents this type of heater. For this particular design each mesh stage is segmented into four identical panels so that a high electrical resistance can be obtained. The current flows through each of the four panels in series before it passes onto the next mesh stage. Electrical insulating material (boron nitride in this case) separates the panels so that each channel directs one-fourth of the gas flow axially through the heater. Since each mesh panel in a stage is identical and the

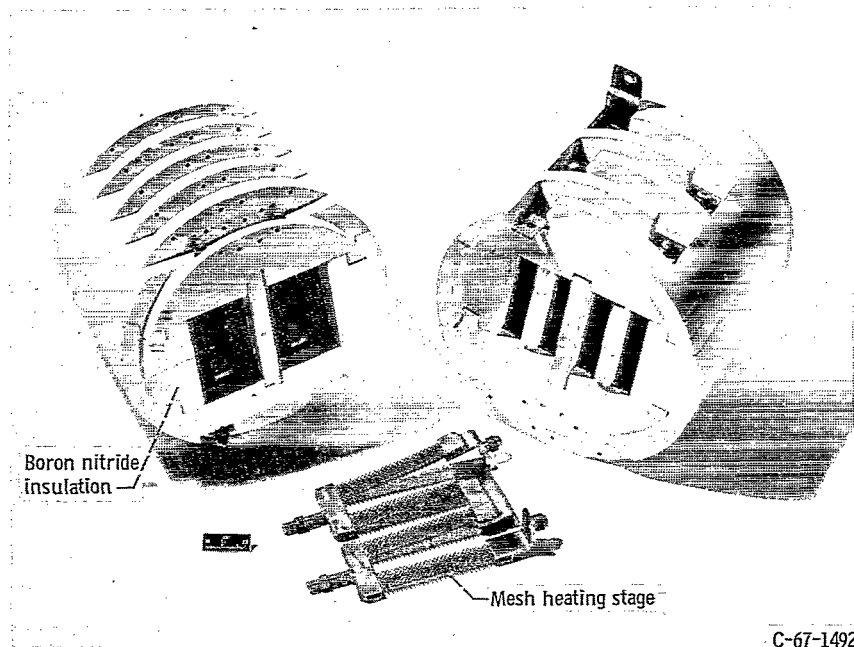


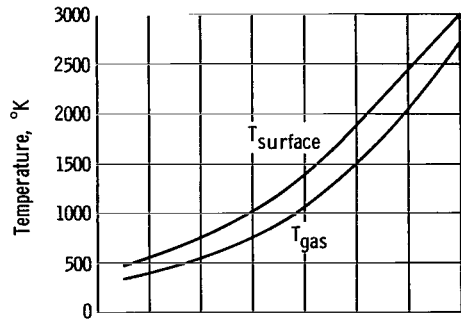
Figure 3. - Series heater.

C-67-1492

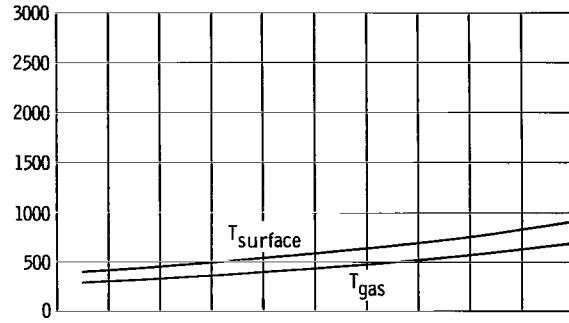
channel flow areas are equal, the heat flux may be assumed equal throughout the stage. The mesh dimensions used were 1.27 centimeters wide by 5.08 centimeters long for each of the four flow passages in one stage for a total mesh frontal area of 25.8 square centimeters per stage.

Figure 4 shows the effect of wire diameter on heater design. The large diameter (0.127 cm) wire mesh has such a low electrical resistance that the heat flux is very small. A heater using this size wire throughout would be prohibitively long to achieve the desired gas temperature. The small diameter (0.036 cm) wire mesh has a much higher electrical resistance with about the same surface area. Consequently, the mesh operates at a higher surface temperature that increases exponentially with heater length. This is caused chiefly by the increase in tungsten resistivity with temperature. The result is a short compact heater in which the major portion of the heat is generated and transferred in the last few stages. This is not a good design because it is susceptible to mesh burnout. The combination of high surface temperature, high heat flux and small, hence weak, wires would probably result in a burnout in the event of any small maldistribution in gas flow through the mesh.

Figure 5 shows the effect of maximizing surface temperature. This was done by choosing mesh from table I that would give the highest electrical resistance for each stage without exceeding  $3200^{\circ}$  K. The result is a very short, compact heater in which the heat flux is very high. Since these heat fluxes have not been demonstrated experi-

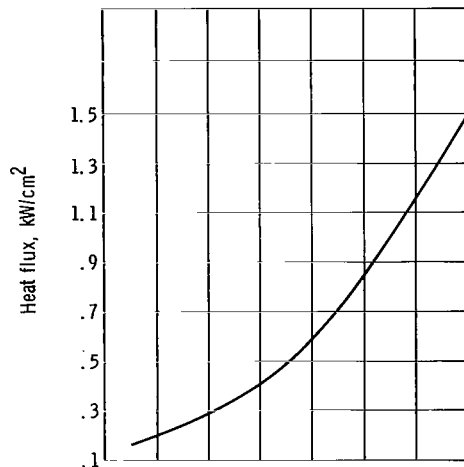


(a-1) Wire diameter, 0.036 centimeter.

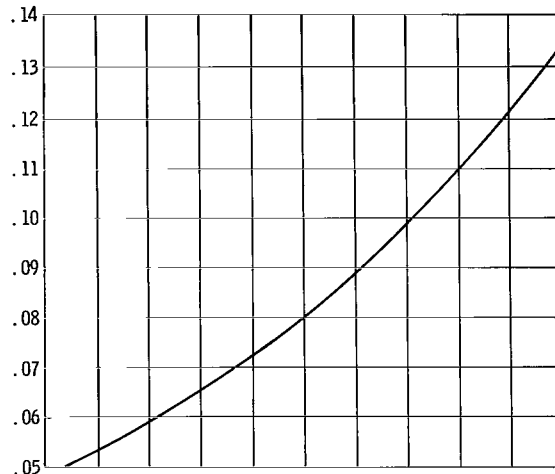


(a-2) Wire diameter, 0.127 centimeter.

(a) Temperature profile.

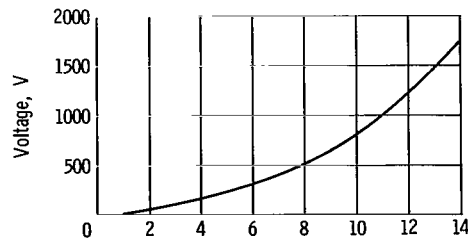


(b-1) Wire diameter, 0.036 centimeter.

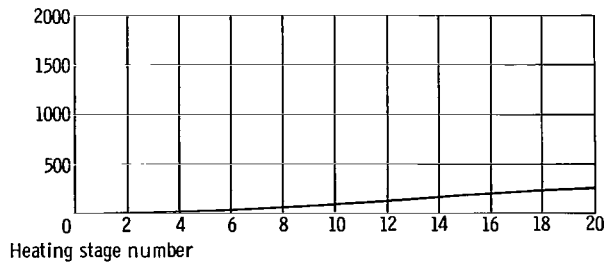


(b-2) Wire diameter, 0.127 centimeter.

(b) Heat flux profile.



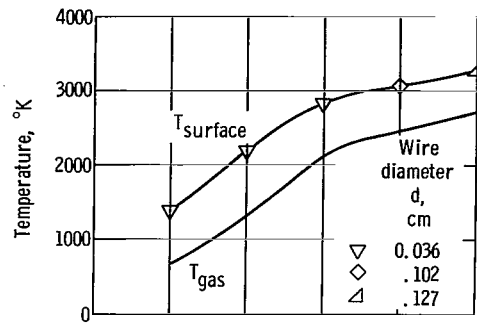
(c-1) Wire diameter, 0.036 centimeter.



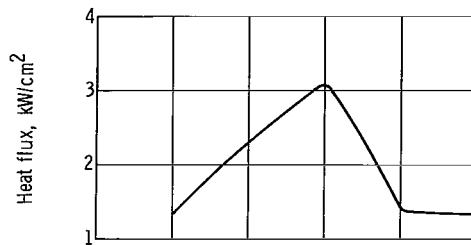
(c-2) Wire diameter, 0.127 centimeter.

(c) Voltage profile.

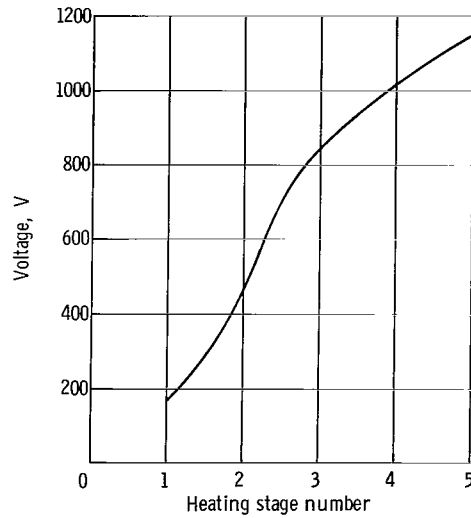
Figure 4. - Effect of wire diameter for high voltage series connected heater. Operating conditions: hydrogen gas; gas flow rate, 0.045 kilogram per second; current, 1000 amperes.



(a) Temperature profile.



(a) Heat flux profile.



(c) Voltage profile.

Figure 5. - Effect of maximizing surface temperature for high voltage series connected heater. Operating conditions: hydrogen gas; gas flow rate, 0.045 kilogram per second; current, 1500 amperes.

mentally, this does not represent a practical design. Another factor that would tend to negate this design would be the high voltage drops across each mesh. For example, the maximum voltage difference between adjacent stages of figure 5 is 682 volts. Providing sufficient insulation to prevent arcing could be a limiting problem, particularly at the peak temperatures.

From the foregoing discussion it may be concluded that a practical series heater design would consist of various meshes that would all operate at a fairly uniform heat flux. The heat flux would be high enough so that the heater dimensions will remain compact but not high enough to cause burnout due to flow maldistribution. The smaller wire diameter mesh would be used at the heater inlet, and as the operating temperature increases the wire size would increase so that the mesh operating at the highest temperature is also the strongest.

## Low Voltage Heater Design

For a constant low voltage, variable high current power supply the mesh heater elements are connected electrically in parallel. Each mesh operates with the same voltage drop but the current through each varies inversely with the resistance. Consequently, the cooler elements carry more current and operate at a higher heat flux than the hotter ones, just the opposite of the series heater.

Figure 6 represents this type of parallel heater. For this analysis the mesh panels are 5.08 centimeters by 5.08 centimeters. The power is introduced through water cooled copper tubes and buses. The heater elements are bolted onto the buses which form two sides of the square flow passage. Insulating material (boron nitride) forms the other two sides of the channel. The gas flows in series through each mesh, increasing in temperature from one stage to the next.

Figure 7 shows the effect of wire diameter on heater design. The low electrical resistance of the large diameter (0.127 cm) wire mesh makes it more compatible with this type of power supply than the small wire diameter mesh. The result is a short heater operating at a high average heat flux with the 0.127-centimeter wire as compared to a long heater operating at a relatively low average heat flux for the 0.036-centimeter wire. In comparing these designs with the series heater it becomes evident that the temperature and heat flux gradients for the parallel heaters are not as severe as those of the series heaters. This is because the parallel electrical connection has an equalizing effect. Since the resistance of each mesh increases with temperature, the current will distribute itself inversely with temperature. Consequently the cooler mesh will carry more current and the hotter ones less for the same applied voltage, thereby flattening the mesh temper-

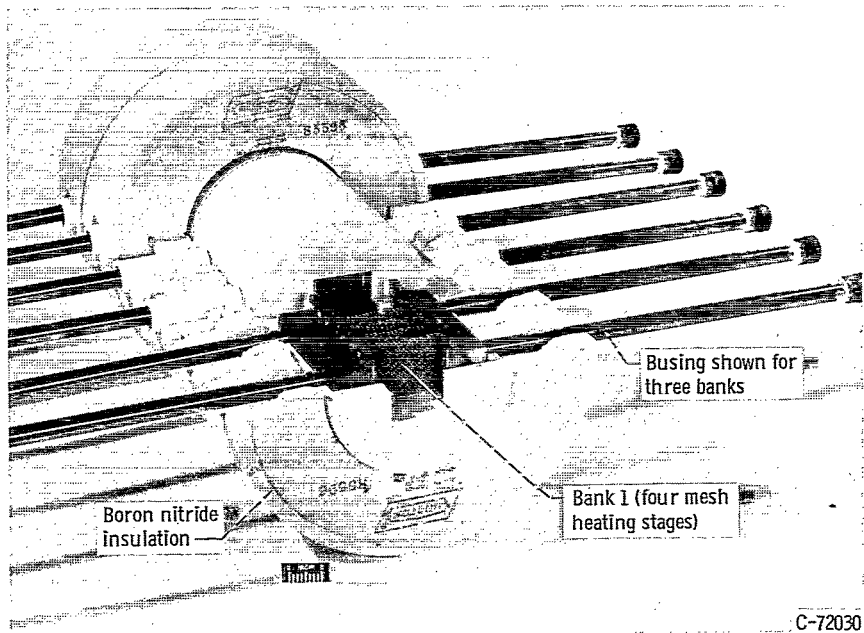
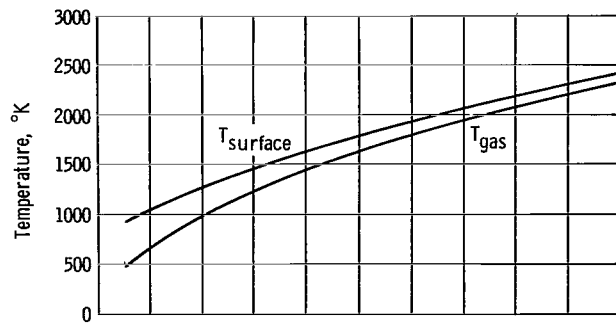
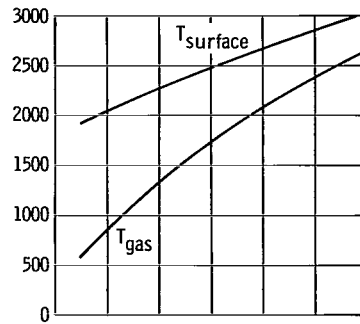


Figure 6. - Parallel heater.



(a-1) Wire diameter, 0.036 centimeter.

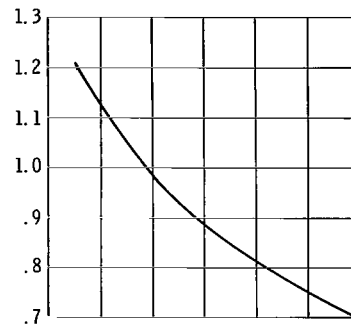


(a-2) Wire diameter, 0.127 centimeter.

(a) Temperature profile.

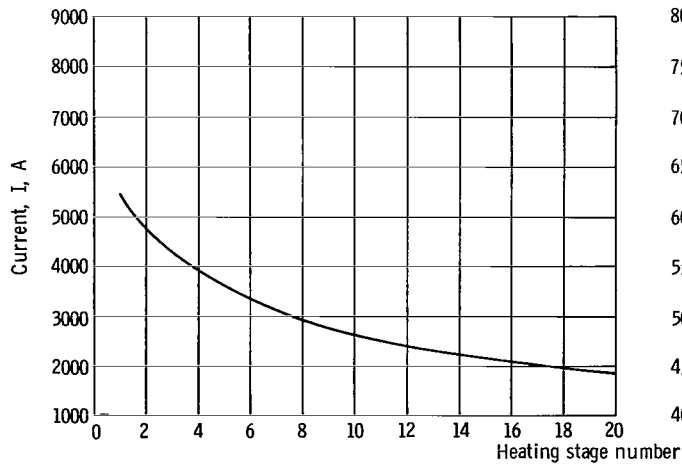


(b-1) Wire diameter, 0.036 centimeter.

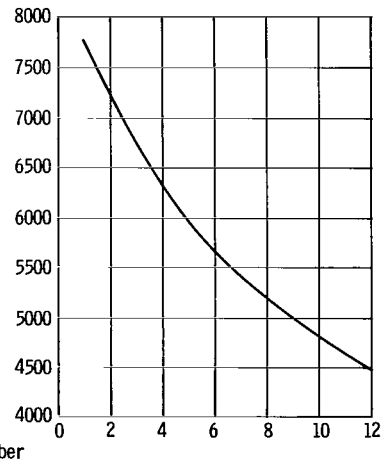


(b-2) Wire diameter, 0.127 centimeter.

(b) Heat flux profile.



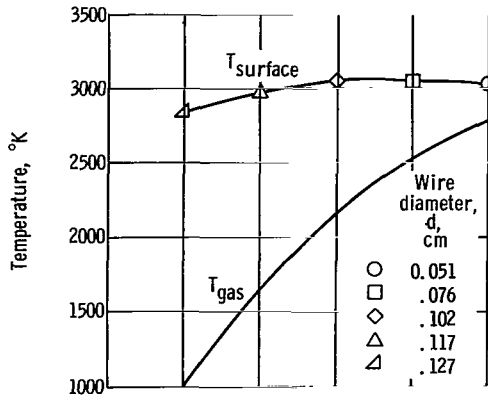
(c-1) Wire diameter, 0.036 centimeter.



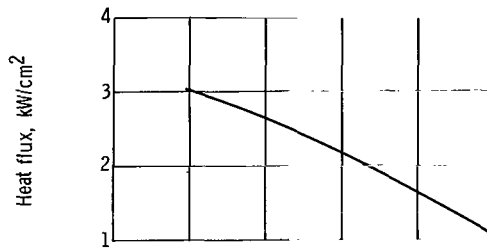
(c-2) Wire diameter, 0.127 centimeter.

(c) Current profile.

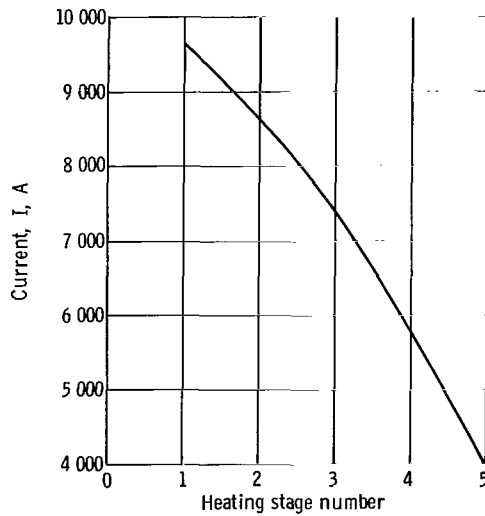
Figure 7. - Effect of wire diameter for high current parallel connected heater. Operating conditions: hydrogen gas; gas flow rate, 0.045 kilogram per second; voltage, 25 volts.



(a) Temperature profile.



(b) Heat flux profile.



(c) Current profile.

Figure 8. - Effect of maximizing surface temperature for high current parallel connected heater. Operating conditions: hydrogen gas; gas flow rate, 0.045 kilogram per second; voltage, 50 volts.

ature profile and to some extent the flux profile. Additional equalization can be achieved by varying the mesh wire diameter.

Figure 8 shows the effect of maximizing surface temperature by tailoring each mesh stage. As with the series heater, the result is a very short compact heater with the mesh operating at very high heat fluxes. In addition to being susceptible to burnout, this design would impose very large demands on the electrical busing. The necessity of delivering 40 000 amperes to these five mesh stages in a small volume of space would be a very difficult design problem.

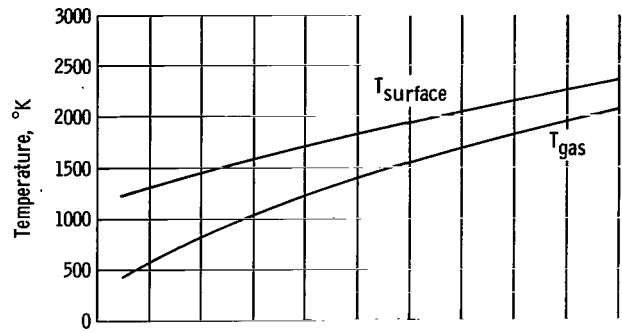
The same general conclusion applies to the parallel heater as for the series heater. The better design is achieved by equalizing the mesh heat flux at some reasonable value and minimizing the number of mesh operating near the maximum allowable surface temperature. Reference 8 represents this type of compromise design.

### Effect of Gas

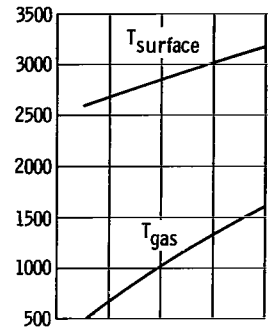
A heater designed for one gas will operate quite differently with another gas. Figure 9 compares nitrogen operation with the parallel heater designs of figure 7. The comparison is made with a nitrogen flow rate that corresponds to the same power and gas temperature rise as for the hydrogen design conditions; that is,

$$W_{N_2} = W_{H_2} \frac{C_{p, H_2}}{C_{p, N_2}} \quad (17)$$

For the same applied voltage, the mesh operate at a higher surface temperature for nitrogen than for hydrogen. This is chiefly because nitrogen has a lower thermal conductivity which causes its heat transfer coefficient to be less than that for hydrogen as seen by equation (10). By comparing thermal conductivities it is possible to predict heater behavior for gases other than the design gas. As in the previous cases, it would be necessary to operate the nitrogen heater at both a lower power level and flow rate to achieve 2780° K gas. However, in order to accurately predict the flow rate and power level, it would be necessary to use the computer program described in appendix B.

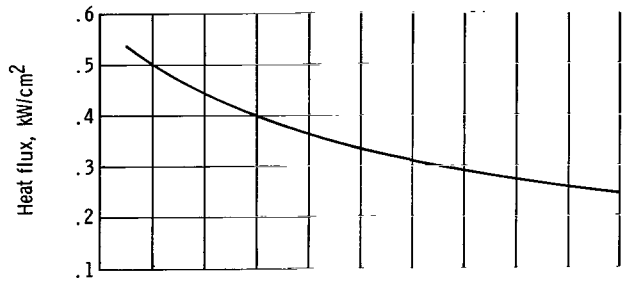


(a-1) Wire diameter, 0.036 centimeter.

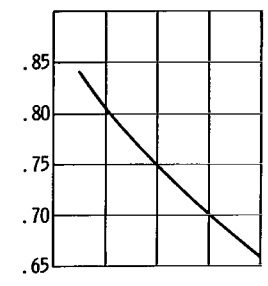


(a-2) Wire diameter, 0.127 centimeter.

(a) Temperature profile.

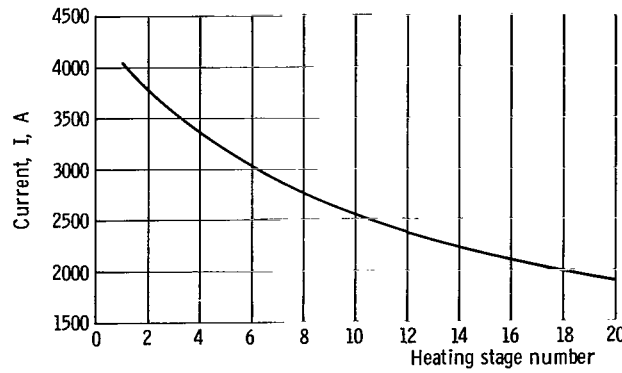


(b-1) Wire diameter, 0.036 centimeter.

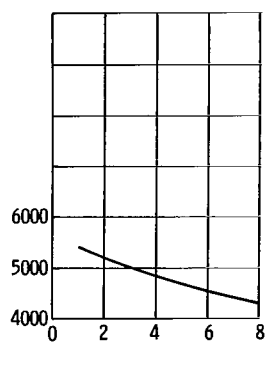


(b-2) Wire diameter, 0.127 centimeter.

(b) Heat flux profile.



(c-1) Wire diameter, 0.036 centimeter.



(c-2) Wire diameter, 0.127 centimeter.

(c) Current profile.

Figure 9. - Effect of nitrogen gas on operation for high current parallel connected heater. Operating conditions: nitrogen gas; gas flow rate, 0.63 kilogram per second; voltage, 25 volts.

## Experimental Results

An electrical resistance wire mesh gas heater has been designed and built with the aid of the analytical program described herein. A detailed description of this heater is presented in reference 9. The heater was originally designed for hydrogen but has been used both as a nitrogen and hydrogen heater. It consists of four banks of mesh stages similar to the three banks shown in figure 6. Each bank represents a different mesh geometry and each is powered by a separate low voltage power supply. The mesh heating elements are connected in parallel as in figure 6. Figure 10 compares experimental results for nitrogen operation with the calculated conditions from the analytical program. The calculated average surface temperatures were 1 to 9 percent higher than the experimental average values determined from resistivity measurements but the calculated and measured outlet gas temperature differed by less than 5 percent. These differences are within experimental error and do not detract from the significance of the analytical results.

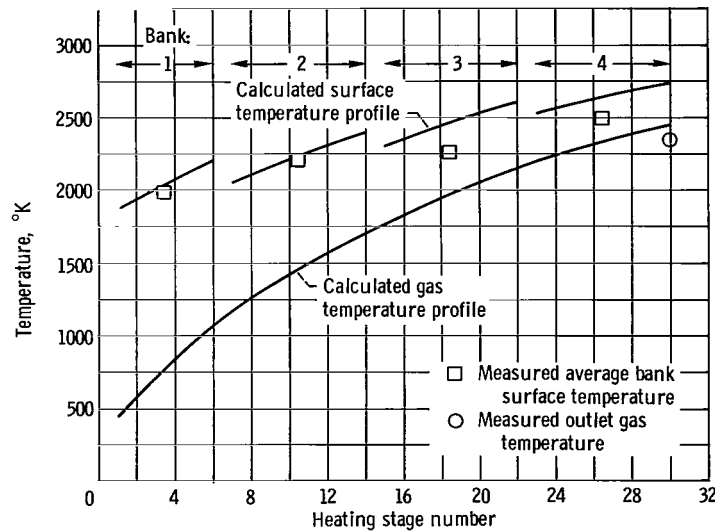


Figure 10. - Comparison of calculated to experimental results for high current parallel connected heater. Operating conditions: nitrogen gas; gas flow rate, 0.313 kilogram per second.

## SUMMARY OF RESULTS

An analytical method is presented whereby an electrical resistance gas heater can be designed using wire mesh as the heating elements. By specifying the type of gas, the flow rate, the system pressure, the desired inlet and outlet temperatures, and a power supply of sufficient capacity and known voltage and current rating, a compatible wire mesh design can be determined. The calculations involve solving simultaneous equations for the heat generation rate, the convective heat transfer from the mesh to the gas, and the change in enthalpy of the gas at every axial position along the heater length.

Wire mesh heating elements provide the designer with compactness and the flexibility to match the heater conditions to practically any type of power supply. For low voltage power supplies, the mesh are connected electrically in parallel while for high voltage power supplies, a series electrical connection is desirable. In both cases the mesh geometry parameters change with heater length to comply with the varying heat transfer conditions throughout the system. High heat fluxes and surface temperatures should be avoided since they increase the chance of mesh burnout because of slight flow maldistributions that are inherent with any porous geometry.

Given specific operating conditions and limiting conditions such as surface temperature and heat flux, the analytical method permits one to optimize the heater design for compactness. It also permits one to determine the operating conditions for the heater when it is used for a different purpose such as with another gas or at some off-design condition with the same gas. Comparing the results from the analysis with actual experimental results of an operating heater demonstrates the usefulness of this analytical method.

Lewis Research Center,  
National Aeronautics and Space Administration,  
Cleveland, Ohio, February 23, 1968,  
120-07-04-54-22.

## APPENDIX A

### SYMBOLS

<p><math>A_c</math> total current cross-sectional area, <math>\text{cm}^2</math></p> <p><math>A_f</math> total frontal area, <math>\text{cm}^2</math></p> <p><math>A_s</math> total surface area, <math>\text{cm}^2</math></p> <p><math>b</math> length of coil, cm</p> <p><math>C</math> coefficient in eq. (10)</p> <p><math>C_p</math> specific heat of gas at constant pressure, <math>\text{J}/(\text{kg})(^\circ\text{K})</math></p> <p><math>D</math> mandrel diameter, cm</p> <p><math>D_e</math> equivalent diameter, cm</p> <p><math>D_t</math> tube diameter, cm</p> <p><math>d</math> wire diameter, cm</p> <p><math>f</math> friction factor</p> <p><math>G</math> average mass velocity, <math>(\text{kg}/\text{sec})/\text{cm}^2</math></p> <p><math>h</math> average heat transfer coefficient, <math>\text{J}/(\text{sec})(\text{cm}^2)(^\circ\text{K})</math></p> <p><math>I</math> current, A</p> <p><math>k</math> thermal conductivity of gas, <math>\text{J}/(\text{cm})(\text{sec})(^\circ\text{K})</math></p> <p><math>L</math> tube length, cm</p>	<p><math>N</math> number of parallel coils</p> <p><math>n</math> exponent in eq. (10)</p> <p><math>p</math> coil pitch, cm/turn</p> <p><math>Q</math> rate of heat transfer to gas, J/sec</p> <p><math>R</math> electrical resistance, ohm</p> <p><math>S</math> total wire length of helical coil, cm</p> <p><math>T_b</math> average bulk temperature, <math>^\circ\text{K}</math></p> <p><math>T_s</math> average surface temperature, <math>^\circ\text{K}</math></p> <p><math>T_w</math> wall temperature, <math>^\circ\text{K}</math></p> <p><math>T_1</math> stage inlet gas temperature, <math>^\circ\text{K}</math></p> <p><math>T_2</math> stage outlet gas temperature, <math>^\circ\text{K}</math></p> <p><math>V</math> voltage, V</p> <p><math>W</math> gas flow rate, kg/sec</p> <p><math>w</math> mesh width, cm</p> <p><math>\epsilon</math> mesh porosity</p> <p><math>\mu</math> absolute viscosity of gas, <math>\text{kg}/(\text{sec})(\text{cm})</math></p> <p><math>\rho</math> resistivity of tungsten, ohm-cm</p>
---	--

## APPENDIX B

### COMPUTER PROGRAM

by Geraldine E. Amling

The computer program presented herein was written for the purpose of designing wire mesh heating elements for an electrical resistance flowing gas heater. If the gas, the flow rate, the system pressure, the desired inlet and outlet gas temperatures, and the power supply characteristics are known, a compatible wire mesh heater element can be determined. Basically, this program solves the following three simultaneous equations having three unknowns, surface temperatures TS, outlet gas temperature T2, and the rate of heat transfer to gas Q: (English units, as defined in the section Computer Code Symbols of this appendix, are used throughout.)

$$Q = \frac{0.948 \times 10^{-3} E^2}{5.2 \times 10^{-6} \left( \frac{TS}{1000} \right)^{1.185} XLA \cdot XL} \quad (B1)$$

$$Q = FR \cdot CP(T2 - T1) \quad (B2)$$

$$Q = \frac{AR}{144} (ASF) \left[ 0.364 \left( \frac{144 FR \cdot DE}{P \cdot AR \cdot XMU} \right)^{0.542} \frac{XK}{DE} \right] \left[ TS - \left( \frac{T1 + T2}{2} \right) \right] \quad (B3)$$

If current is to be specified instead of voltage, equation (B1) would be changed to

$$Q = I^2 (5.2 \times 10^{-6}) \left( \frac{TS}{1000} \right)^{1.185} (XLA)(XL) \quad (B4)$$

The resistivity of tungsten,  $5.2 \times 10^{-6} (TS/1000)^{1.185}$ , is from reference 6. Since the Prandtl number in reference 1 is nearly a constant, it was not included in the correlation presented in equation (B3). The method used to solve these equations was the Newton-Raphson iteration process (ref. 7) with Gauss double precision routine to solve the matrix. For the specific case presented, gas properties are evaluated at the mesh surface temperature; however, evaluation could be at any specified temperature with only minor changes to the program. The solution requires an initial estimate of TS, Q, and T2 in the region of convergence of the functions used. Corrections are then repeatedly calculated and added to the values until the desired accuracy is obtained. If AH, AL, and

AK are corrections to the initial estimate for Q, T2, and TS, respectively, then

$$Q1 + AH = Q' 1 \quad (B5)$$

$$T2 + AL = T' 2 \quad (B6)$$

$$TS + AK = T' S \quad (B7)$$

The new, more exact values are then used to calculate new corrections.

In the program, preliminary estimates of starting values are obtained by using a single iterative process to determine, within  $100^{\circ}$  R, the value of TS, and the corresponding values of T2 and Q. The approximation is further refined using the subroutine MGAUSD to obtain a TS value which is within 1 percent of the true value.

Starting values used in this program are approximations, and although satisfactory results were obtained in all cases run, there is a possibility that the Newton-Raphson method will not converge for a given set of values.

Hydrogen, nitrogen, and helium properties have been curve fitted in the range of  $500^{\circ}$  to  $6000^{\circ}$  R. The coefficients of the curves are included in the main program as data, where the units of these properties are as follows:

Temperature,  $^{\circ}$ R; thermal conductivity XK, Btu/(ft)(sec)( $^{\circ}$ R); viscosity XMU, lb/(ft)(sec); specific heat CP, Btu/(lb)( $^{\circ}$ R).

If the surface temperature TS becomes negative, a print out of TS is given, computation is terminated. and program reads in a new case.

Accuracy of the approximations using Newton-Raphson technique was established by convergence of Q values at the 1.0 percent level. However, the percent error may be increased or decreased according to the user's needs. Percent error tests are made at statement number 14 and statement number 16. If specified accuracy is not achieved after 50 iterations, a print out of TS, T2, and Q is given, computation is terminated, and program reads in a new case.

## Input

The input format sheet is shown in table II. The quantities filled in are for a sample problem. The output for this sample problem will be presented subsequently.



Instructions for preparing the input are given in table III.

TABLE III. - INSTRUCTIONS FOR PREPARING INPUT

Card type	Number	Columns	Description of variables	
1	1	1 to 2	CODE	two-letter code for type gas (H2, HE, or N2)
		3 to 4	NN	number of stage groups
2 (constants for each stage)	NN	1 to 8	D	wire diameter, in.
		9 to 16	E	voltage, V
		17 to 24	ASF	$A_s/A_f$ , total surface area/total frontal area
		25 to 31	DE	equivalent diameter, ft
		33 to 40	P	mesh porosity, percent
		41 to 48	XLA	$S/A_c$ , total wire length/total current cross-sectional area (for 1 sq in. of mesh)
		49 to 56	XIT	last mesh number of each stage
3 (data for one case)	1	1 to 8	PCE	percent error
		9 to 16	AR	total frontal area, in. <sup>2</sup>
		17 to 24	XL	mesh length/mesh width
		25 to 32	FR	gas flow rate, lb/sec
		33 to 40	T11	$T_1$ , stage inlet gas temperature, °R

Card type number 2 may be repeated for a group of stages (NN). The sample problem has a total of 30 stages. The first group contains 6 stages (XIT(1) = 6.0); the second group, 8 stages (XIT(2) = 14.0); the third group, 8 stages (XIT(3) = 22.0); and the fourth group contains 8 stages (XIT(NN) = 30.0).

This program is written in FORTRAN IV and is operational on the IBM 7094-2/7044 direct-coupled system of the Lewis Research Center. A flow chart of the program is shown in figure 11.

Machine running time is approximately 2 minutes per case.

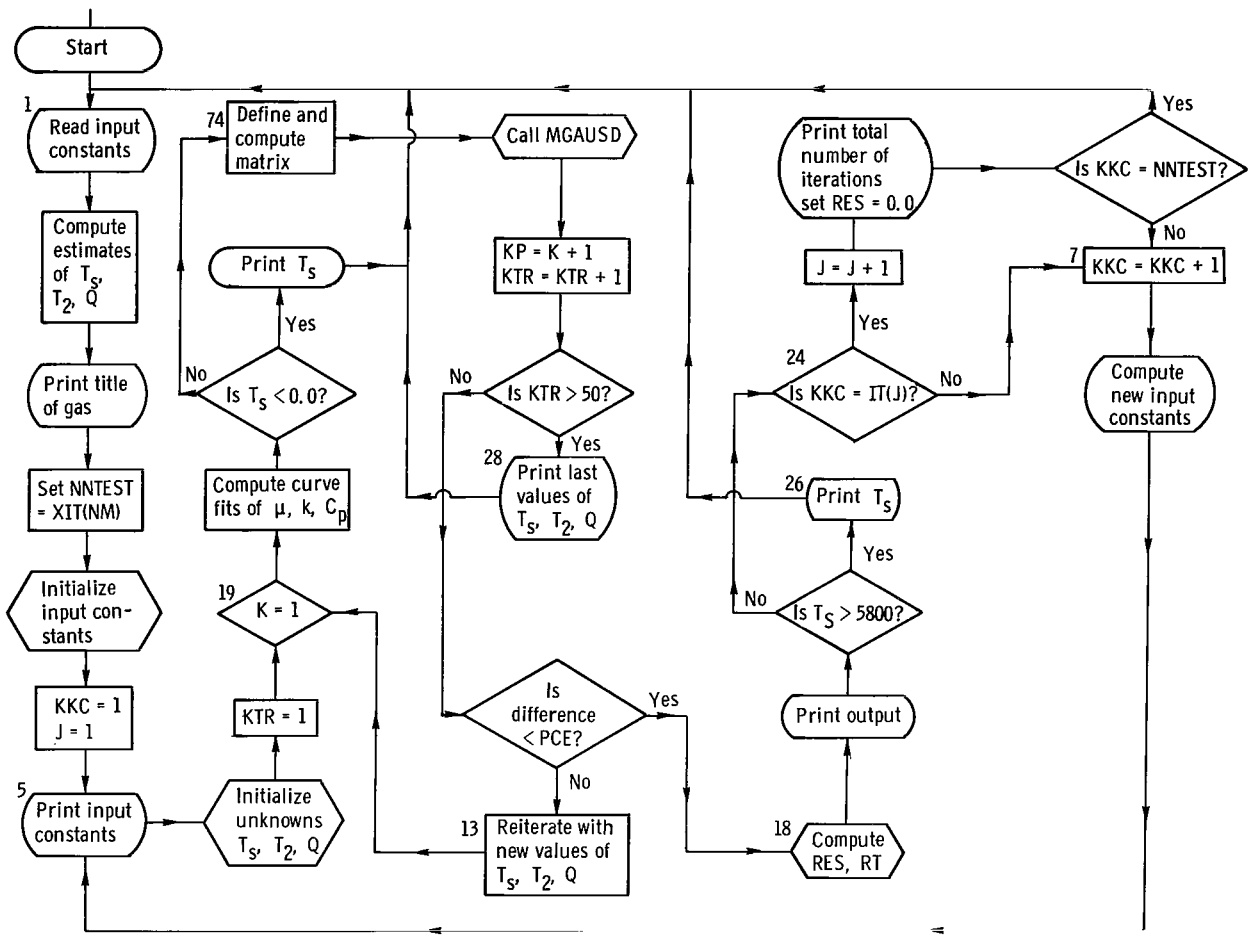


Figure 11. - Flow chart for main program HEWMAN.

## Output

Input and output are printed out for each iteration. Output consists of the following:

T2	outlet gas temperature, °R
TS	surface temperature, °R
Q	rate of heat transfer to gas, Btu/sec
RT	total resistance
IT	mesh number

## Computer Code Symbols

A1	first equation (B1)
A2	second equation (B2)
A3	third equation (B3)
AH	correction factor for Q
AK	correction factor for $T_s$
AL	correction factor for $T_2$
AR	$A_f$ , total frontal area, in. <sup>2</sup>
ASF	$A_s/A_f$ , total surface area/total frontal area, in. <sup>2</sup> /in. <sup>2</sup>
CODE	two letter code for element (H <sub>2</sub> , He, or N <sub>2</sub> )
CP	specific heat of gas at constant pressure, Btu/(lb)(°R)
CPA	current coefficients, $C_p$ curve, at T11
CPAH	coefficients, $C_p$ curve, hydrogen
CPAHE	coefficients, $C_p$ curve, helium
CPAN	coefficients, $C_p$ curve, nitrogen
CPBPH	breaking points, $C_p$ curve, hydrogen
CPBPHE	breaking points, $C_p$ curve, helium
CPBPN	breaking points, $C_p$ curve, nitrogen
CTS	current value of $T_s$
D	d, wire diameter, in.

DCP	derivative of $C_p$ at T11
DE	$D_e$ , equivalent diameter, ft
DK	derivative of $k$ at CTS
DM	derivative of $\mu$ at CTS
DRES	reciprocal of electrical resistance at each stage, ohm
E	voltage, V
FR	W, gas flow rate, lb/sec
IT	XIT, mesh number
KKC	stage number
L	denotes gas used
NN	number of stage groups
NNTEST	last stage of each case
P	$\epsilon$ , mesh porosity, percent
PCE	percent error
Q	rate of heat transfer to gas, Btu/sec
QQQ	initialization of Q
RES	$1/RT$ , reciprocal of electrical resistance
RHO	$\rho$ , resistivity of tungsten, ohm-ft
RT	total electrical resistance, ohm
TB	$T_b = (T_1 + T_2)/2$ , average bulk temperature, $^{\circ}R$
TS	$T_s$ , average surface temperature, $^{\circ}R$
TS1	initialization of $T_s$
T11	initial $T_1$ , stage inlet gas temperature, $^{\circ}R$
T2	stage outlet gas temperature, $^{\circ}R$
T21	initialization of $T_2$
XIT	mesh number
XK	$k_g$ , thermal conductivity of gas, Btu/(ft)(sec)( $^{\circ}R$ )
XKA	current coefficients, k curve, at CTS
XKAH	coefficients, k curve, hydrogen

XKAHE coefficients, k curve, helium  
 XKAN coefficients, k curve, nitrogen  
 XKBPHE break points, k curve, helium  
 XKBPHE break points, k curve, helium  
 XKBPHE break points, k curve, helium  
 XKBPHE break points, k curve, nitrogen  
 XL mesh length/mesh width  
 XLA  $S/A_c$ , total wire length/total cross-sectional area (for 1 sq in. of mesh)  
 XM  $\mu$  at CTS  
 XMA current coefficients,  $\mu$  curve, at CTS  
 XMAH coefficients,  $\mu$  curve, hydrogen  
 XMAHE coefficients,  $\mu$  curve, helium  
 XMAN coefficients,  $\mu$  curve, nitrogen  
 XMBPH break points,  $\mu$  curve, hydrogen  
 XMBPHE break points,  $\mu$  curve, helium  
 XMBPHE break points,  $\mu$  curve, helium  
 XMBPHE break points,  $\mu$  curve, nitrogen  
 XMU  $\mu_s$ , absolute viscosity of gas, lb/(sec)(ft)

## PROGRAM LISTING

```

                                - HEWMAN -                0003
                                HEATED WIRE MESH ANALYSIS  0004
$IBFTC HEWMAN                HEWM0000
C                              HEWM0001
C    ANALYTICAL INVESTIGATION OF ELECTRICALLY HEATED WIRE MESH FOR FLOWHEWM0002
C    ING GAS HEATERS                HEWM0003
C                              HEWM0004
    DIMENSION A(20,21),ANS(20),D(35),ASF(35),DE(35),A1(2),A2(2),A3(2),HEWM0005
    1T2(2),TS(2),Q(2),RHO(2),TB(2),P(35),TTS(35),TT2(35),QQQ(35),DRES(3HEWM0006
    25),QIN(35),XLA(35),E(35),XIT(35),IT(35),TITLE(6),TEST(3),CPBPH(3),HEWM0007
    3CPAH(3,5),XKBPH(4),XKAH(4,5),XMBPH(2),XMAH(2,5),CPBPHE(1),CPAHE(1,HEWM0008
    45),XKBPHE(5),XKAHE(5,5),XMBPHE(5),XMAHE(5,5),CPBPN(3),CPAN(3,5),XKHEWM0009
    5BPN(3),XKAN(3,5),XMBPN(2),XMAN(2,5),CPA(5),XKA(5),XMA(5),QG(2)  HEWM0010
    DOUBLE PRECISION A,ANS                HEWM0011
    DATA TITLE/6HHYDROG,3HEN ,6HHELIUM,3H    ,6HNITROG,3HEN /    HEWM0012
    DATA TEST/2HH2,2HHE,2HN2/                HEWM0013
C                              HEWM0014
C    CURVE FIT COEFFICIENTS                HEWM0015
C                              HEWM0016
    DATA(CPBPH(I),(CPAH(I,J),J=1,5),I=1,3)/1600.,.60895594E-13,-.17668HEWM0017
    1624E-09,.19863776E-06,-.58512098E-04,.34488570E+01,3400.,.66711351HEWM0018
    2E-14,-.96354453E-10,.47186254E-06,-.68641899E-03,.37794389E+01,999HEWM0019
    39.,.33788127E-14,-.54401793E-10,.29369051E-06,-.40627483E-03,.3680HEWM0020
    43507E+01/                HEWM0021
    DATA(XKBPH(I),(XKAH(I,J),J=1,5),I=1,4)/3240.,-.44762447E-18,.45602HEWM0022
    1272E-14,-.14757960E-10,.49758692E-07,.67895535E-05,4200.,-.2244840HEWM0023
    24E-17,.19534089E-13,-.14034318E-10,-.20252412E-06,.50636788E-03,50HEWM0024
    300.,.13421374E-17,-.79444732E-14,-.15509958E-10,.21192557E-06,-.28HEWM0025
    4865473E-03,9999.,.31153528E-18,.14254711E-14,-.79974343E-11,-.5965HEWM0026
    59474E-07,.35433426E-03/                HEWM0027
    DATA(XMBPH(I),(XMAH(I,J),J=1,5),I=1,2)/3240.,-.41257712E-19,.46966HEWM0028
    1670E-15,-.21505826E-11,.91476697E-08,.16277624E-05,9999.,.16330742HEWM0029
    2E-19,-.23379722E-15,.12630465E-11,.13345724E-08,.86894117E-05/    HEWM0030
    DATA(CPBPHE(I),(CPAHE(I,J),J=1,5),I=1,1)/9999.,0.0,0.0,0.0,0.0,1.2HEWM0031
    148/                HEWM0032
    DATA(XKBPHE(I),(XKAHE(I,J),J=1,5),I=1,5)/1080.,-.77890956E-17,.277HEWM0033
    180897E-13,-.42174067E-10,.56632175E-07,.35187003E-05,1980.,-.10875HEWM0034
    2264E-18,.14469528E-14,-.75917067E-11,.35675647E-07,.85407794E-05,3HEWM0035
    3060.,.22115952E-18,-.20091672E-14,.54316253E-11,.14383910E-07,.213HEWM0036
    499514E-04,4320.,.99375672E-18,-.14409781E-13,.77161781E-10,-.16520HEWM0037
    5692E-06,.18686650E-03,9999.,.10734377E-18,-.18710445E-14,.11455015HEWM0038
    6E-10,-.14133485E-07,.58283775E-04/                HEWM0039
    DATA(XMBPHE(I),(XMAHE(I,J),J=1,5),I=1,5)/1080.,-.43709039E-17,.154HEWM0040
    162508E-13,-.23183404E-10,.30621850E-07,.18674307E-05,1980.,-.49656HEWM0041
    2867E-18,.34463889E-14,-.10082049E-10,.25066486E-07,.24508796E-05,3HEWM0042
    3060.,.96140067E-19,-.80792886E-15,.17373264E-11,.99491831E-08,.996HEWM0043
    406022E-05,4320.,.69156058E-19,-.97000761E-15,.46564625E-11,-.37171HEWM0044
    5825E-09,.21218701E-04,9999.,.45480686E-19,-.90894728E-15,.65060669HEWM0045

```

```

6E-11,-.12201804E-07,.41129947E-04/                                HEWM0046
  DATA(CPBPN(I),(CPAN(I,J),J=1,5),I=1,3)/1200.,-.32947199E-13,.11359HEWM0047
1297E-09,-.11757656E-06,.51070120E-04,.24025236,2600.,-.38860908E-1HEWM0048
24,.27320397E-10,-.76523934E-07,.12770844E-03,.17811544,9999.,.3465HEWM0049
39852E-15,-.52774543E-11,.27527779E-07,-.49201293E-04,.31484032/  HEWM0050
  DATA(XKBPN(I),(XKAN(I,J),J=1,5),I=1,3)/1900.,-.42173368E-18,.22349HEWM0051
1799E-14,-.44977566E-11,.90421007E-08,.35708245E-06,3800.,.48366958HEWM0052
2E-19,-.55485031E-15,.20306218E-11,.16420137E-08,.38586614E-05,9999HEWM0053
3.,-.58176164E-19,.10634372E-14,-.73856933E-11,.26436289E-07,-.2095HEWM0054
49671E-04/                                HEWM0055
  DATA(XMBPN(I),(XMAN(I,J),J=1,5),I=1,2)/1800.,-.96213327E-18,.52937HEWM0056
1485E-14,-.12553952E-10,.25208125E-07,.11203481E-05,9999.,-.1637768HEWM0057
23E-19,.29989957E-15,-.23507248E-11,.15825006E-07,.41787548E-05/  HEWM0058
C      READ INPUT                                HEWM0059
C      READ (5,107) CODE,NN                        HEWM0060
C      READ (5,100) (D(I),E(I),ASF(I),DE(I),P(I),XLA(I),XIT(I),I=1,NN) HEWM0061
1 READ (5,107) CODE,NN                            HEWM0062
  READ (5,100) (D(I),E(I),ASF(I),DE(I),P(I),XLA(I),XIT(I),I=1,NN) HEWM0063
  READ (5,100) PCE,AR,XL,FR,T11                    HEWM0064
C      PRINT TITLE                                HEWM0065
C      PRINT TITLE                                HEWM0066
C      PRINT TITLE                                HEWM0067
L=0                                                HEWM0068
DO 8 I=1,6,2                                       HEWM0069
L=L+1                                              HEWM0070
IF(CODE.NE.TEST(L)) GO TO 8                        HEWM0071
II=I+1                                             HEWM0072
WRITE (6,101) (TITLE(J),J=I,II)                  HEWM0073
III=II/2                                           HEWM0074
8 CONTINUE                                         HEWM0075
C      STARTING VALUES FOR NEWTON-RAPHSON        HEWM0076
C      STARTING VALUES FOR NEWTON-RAPHSON        HEWM0077
C      STARTING VALUES FOR NEWTON-RAPHSON        HEWM0078
TSG=1500.                                          HEWM0079
T1G=T11                                           HEWM0080
I111=1                                             HEWM0081
97 RHOG=5.2E-6*(TSG*1.0E-3)**1.185               HEWM0082
  QG(1)=(E(1)**2*.948E-3)/(RHOG*XLA(1)*XL)      HEWM0083
  GO TO (90,91,92),I111                          HEWM0084
90 CPG=3.47                                        HEWM0085
  GO TO 93                                         HEWM0086
91 CPG=1.248                                       HEWM0087
  GO TO 93                                         HEWM0088
92 CPG=.248                                         HEWM0089
93 T2G=(QG(1)+CPG*T1G*FR)/(FR*CPG)              HEWM0090
  TBG=(T1G+T2G)/2.0                               HEWM0091
  CTS=TSG                                          HEWM0092
  GO TO 94                                         HEWM0093
95 XG1=(FR*144.0*DE(1))/(P(1)*AR*XM)            HEWM0094
  XG2=(AR*ASF(1)*.364)/(144.0*DE(1))            HEWM0095

```

```

          QG(2)=XG2*XK*(TSG-TBG)*XG1** .542
          IF(QG(2).GT.QG(1)) GO TO 96
          TSG=TSG+100.
          IF(TSG.LT.5800.) GO TO 97
          TSG=1500.
          T2G=600.
          QG(2)=1.0
96      TSIN=TSG
          T2IN=T2G
          IIII=0
          DO 98 I=1,NN
          QIN(I)=QG(2)
98      CONTINUE
          NNTEST=XIT(NN)
          RES=0.0
          T2I=T2IN
          TS1=TSIN
          DO 3 I=1,NN
          QQQ(I)=QIN(I)
3      CONTINUE
          KKC=1
          J=1
C
C      PRINT INPUT FOR EACH STAGE
C
5      WRITE (6,102) KKC
          WRITE (6,106)
          WRITE (6,103)
          WRITE (6,104) D(J),E(J),ASF(J),DE(J),XL,P(J),AR
          WRITE (6,109)
          WRITE (6,104) FR,PCE,T11,XLA(J),T21,TS1,QQQ(J)
          WRITE (6,108)
          T1=T11
          T2(1) = T21
          TS(1) = TS1
          Q(1)= QQQ(J)
          KTR=1
19     K=1
C
C      PROPERTIES OF ELEMENTS COMPUTED
C
          GO TO (40,41,42),IIII
40     DO 43 I1=1,3
          IF(T1.GT.CPBPH(I1))GO TO 43
          DO 44 J1=1,5
          CPA(J1)=CPAH(I1,J1)
44     CONTINUE
          GO TO 49
43     CONTINUE
          WRITE (6,114) T1

```

```

HEWM0096
HEWM0097
HEWM0098
HEWM0099
HEWM0100
HEWM0101
HEWM0102
HEWM0103
HEWM0104
HEWM0105
HEWM0106
HEWM0107
HEWM0108
HEWM0109
HEWM0110
HEWM0111
HEWM0112
HEWM0113
HEWM0114
HEWM0115
HEWM0116
HEWM0117
HEWM0118
HEWM0119
HEWM0120
HEWM0121
HEWM0122
HEWM0123
HEWM0124
HEWM0125
HEWM0126
HEWM0127
HEWM0128
HEWM0129
HEWM0130
HEWM0131
HEWM0132
HEWM0133
HEWM0134
HEWM0135
HEWM0136
HEWM0137
HEWM0138
HEWM0139
HEWM0140
HEWM0141
HEWM0142
HEWM0143
HEWM0144
HEWM0145

```

GO TO 1	HEWM0146
41 DO 45 J1=1,5	HEWM0147
IF(T1.GT.CPBPHE(1)) GO TO 48	HEWM0148
CPA(J1)=CPAHE(1,J1)	HEWM0149
45 CONTINUE	HEWM0150
GO TO 49	HEWM0151
48 WRITE(6,115)T1	HEWM0152
GO TO 1	HEWM0153
42 DO 46 I1=1,3	HEWM0154
IF(T1.GT.CPBPN(I1))GO TO 46	HEWM0155
DO 47 J1=1,5	HEWM0156
CPA(J1)=CPAN(I1,J1)	HEWM0157
47 CONTINUE	HEWM0158
GO TO 49	HEWM0159
46 CONTINUE	HEWM0160
WRITE (6,116) T1	HEWM0161
49 CP=0.0	HEWM0162
DO 50 II=1,5	HEWM0163
CP=CP*T1+CPA(II)	HEWM0164
50 CONTINUE	HEWM0165
CTS = TS(K)	HEWM0166
94 GO TO (51,52,53),III	HEWM0167
51 DO 55 I1=1,4	HEWM0168
IF(CTS.GT.XKBPHE(I1)) GO TO 55	HEWM0169
DO 56 J1=1,5	HEWM0170
XKA(J1)=XKAH(I1,J1)	HEWM0171
56 CONTINUE	HEWM0172
GO TO 59	HEWM0173
55 CONTINUE	HEWM0174
WRITE(6,117) CTS	HEWM0175
GO TO 1	HEWM0176
52 DO 57 I1=1,5	HEWM0177
IF(CTS.GT.XKBPHE(I1)) GO TO 57	HEWM0178
DO 58 J1=1,5	HEWM0179
XKA(JI)=XKAHE(I1,J1)	HEWM0180
58 CONTINUE	HEWM0181
GO TO 59	HEWM0182
57 CONTINUE	HEWM0183
WRITE (6,118) CTS	HEWM0184
GO TO 1	HEWM0185
53 DO 60 I1=1,3	HEWM0186
IF(CTS.GT.XKBPHE(I1)) GO TO 60	HEWM0187
DO 61 J1=1,5	HEWM0188
XKA(J1)=XKAN(I1,J1)	HEWM0189
61 CONTINUE	HEWM0190
GO TO 59	HEWM0191
60 CONTINUE	HEWM0192
WRITE(6,119) CTS	HEWM0193
GO TO 1	HEWM0194
59 XK=0.0	HEWM0195

DK=0.0	HEWM0196
DO 62 II=1,5	HEWM0197
XK=XK*CTS+XKA(II)	HEWM0198
IF(II.EQ.5) GO TO 62	HEWM0199
DK=DK*CTS+XKA(II)*FLOAT(5-II)	HEWM0200
62 CONTINUE	HEWM0201
GO TO (63,64,65),III	HEWM0202
63 DO 66 I1=1,2	HEWM0203
IF(CTS.GT.XMBPH(I1)) GO TO 66	HEWM0204
DO 67 J1=1,5	HEWM0205
XMA(J1)=XMAH(I1,J1)	HEWM0206
67 CONTINUE	HEWM0207
GO TO 69	HEWM0208
66 CONTINUE	HEWM0209
WRITE(6,120) CTS	HEWM0210
GO TO 1	HEWM0211
64 DO 68 I1=1,5	HEWM0212
IF(CTS.GT.XMBPHE(I1)) GO TO 68	HEWM0213
DO 70 J1=1,5	HEWM0214
XMA(J1)=XMAHE(I1,J1)	HEWM0215
70 CONTINUE	HEWM0216
GO TO 69	HEWM0217
68 CONTINUE	HEWM0218
WRITE(6,121) CTS	HEWM0219
GO TO 1	HEWM0220
65 DO 71 I1=1,2	HEWM0221
IF(CTS.GT.XMBPN(I1)) GO TO 71	HEWM0222
DO 72 J1=1,5	HEWM0223
XMA(J1)=XMAN(I1,J1)	HEWM0224
72 CONTINUE	HEWM0225
GO TO 69	HEWM0226
71 CONTINUE	HEWM0227
WRITE(6,122) CTS	HEWM0228
GO TO 1	HEWM0229
69 XM=0.0	HEWM0230
DM=0.0	HEWM0231
DO 73 II=1,5	HEWM0232
XM=XM*CTS+XMA(II)	HEWM0233
IF(II.EQ.5) GO TO 73	HEWM0234
DM=DM*CTS+XMA(II)*FLOAT(5-II)	HEWM0235
73 CONTINUE	HEWM0236
IF(IIII.EQ.1) GO TO 95	HEWM0237
IF(TS(K).GT.0.0) GO TO 74	HEWM0238
WRITE(6,123) TS(K)	HEWM0239
GO TO 1	HEWM0240
C	HEWM0241
C	HEWM0242
C	HEWM0243
74 RHO(K) = 5.2E-6*(TS(K)/1000.0)**1.185	HEWM0244
A1(K) = ((E(J)**2*.948E-3)/(RHO(K)*XLA(J)*XL))-Q(K)	HEWM0245

```

A2(K) = FR*CP*(T2(K)-T1)-Q(K) HEWM0246
TB(K) = (T1+T2(K))/2.0 HEWM0247
XCON1=(FR*144.*DE(J))/(P(J)*AR*XM) HEWM0248
XCON2=(AR*ASF(J)*.364)/(144.*DE(J)) HEWM0249
A3(K)=(XCON2*XK*(TS(K)-TB(K))*XCON1** .542)-Q(K) HEWM0250
DA=XCON2*(XK+DK*(TS(K)-TB(K))) HEWM0251
DB=(.542/(XCON1** .458))*((-XCON1*DM)/XM) HEWM0252
DO 30 II=1,3 HEWM0253
DO 30 M=1,4 HEWM0254
A(II,M)=0.0D0 HEWM0255
30 CONTINUE HEWM0256
A(1,1) = -1.0 HEWM0257
A(2,1) = -1.0 HEWM0258
A(3,1) = -1.0 HEWM0259
A(1,2) = (-1.185*E(J)**2*.948E-3*(1.0/TS(K)**2.185)*1000.0**1.185) HEWM0260
2/(5.2E-6*XLA(J)*XL) HEWM0261
A(2,2) = 0.0 HEWM0262
A(3,2) = XCON2*XK*(TS(K)-TB(K))*DB+XCON1** .542*DA HEWM0263
A(1,3) = 0.0 HEWM0264
A(2,3) = FR*CP HEWM0265
A(3,3) = -.5*XCON2*XK*XCON1** .542 HEWM0266
A(1,4) = -A1(K) HEWM0267
A(2,4) = -A2(K) HEWM0268
A(3,4) = -A3(K) HEWM0269
CALL MGAUSD(A,3,ANS) HEWM0270
AH=ANS(1) HEWM0271
AK = ANS(2) HEWM0272
AL = ANS(3) HEWM0273
KP=K+1 HEWM0274
Q(KP)=Q(K)+AH HEWM0275
TS(KP)=TS(K)+AK HEWM0276
T2(KP)=T2(K)+AL HEWM0277
TESTQ=ABS((Q(1)-Q(2))/Q(2)) HEWM0278
TESTTS=ABS((TS(1)-TS(2))/TS(2)) HEWM0279
TESTT2=ABS((T2(1)-T2(2))/T2(2)) HEWM0280
KTR=KTR+1 HEWM0281
IF(KTR.GT.50) GO TO 28 HEWM0282
IF(TESTQ-PCE) 14,13,13 HEWM0283
14 IF(TESTTS-PCE) 16,13,13 HEWM0284
16 IF(TESTT2-PCE) 18,13,13 HEWM0285
13 Q(1)=Q(2) HEWM0286
TS(1)=TS(2) HEWM0287
T2(1)=T2(2) HEWM0288
GO TO 19 HEWM0289
18 TTS(J)=TS(2) HEWM0290
TT2(J)=T2(2) HEWM0291
QQQ(J)=Q(2) HEWM0292
RHO(2)=5.2E-6*(TS(2)/1000.0)**1.185 HEWM0293
DRES(J)=1.0/(XLA(J)*RHO(2)*XL) HEWM0294
RES=RES+DRES(J) HEWM0295

```

	RT=1.0/RES	HEWM0296
C		HEWM0297
C	PRINT OUTPUT FOR EACH STAGE	HEWM0298
C		HEWM0299
	WRITE (6,105)	HEWM0300
	WRITE (6,104) T2(2),TS(2),Q(2),RT	HEWM0301
	IF(TTS(J).LE.5800.0) GO TO 24	HEWM0302
26	WRITE(6,111)	HEWM0303
	GO TO 1	HEWM0304
24	IT(J)=XIT(J)	HEWM0305
	IF(KKC.NE.IT(J)) GO TO 7	HEWM0306
	WRITE(6,112) IT(J)	HEWM0307
	WRITE(6,126)	HEWM0308
	RES=0.0	HEWM0309
	IF(IT(J).EQ.NNTEST) GO TO 1	HEWM0310
7	KKC=KKC+1	HEWM0311
	TS1=TTS(J)	HEWM0312
	T21=TT2(J)+(TT2(J)-T1)	HEWM0313
	T11=TT2(J)	HEWM0314
	IF(KKC.GT.IT(J)) J=J+1	HEWM0315
	GO TO 5	HEWM0316
28	WRITE (6,113)	HEWM0317
	WRITE(6,124) TS(1),TS(2),T2(1),T2(2),Q(1),Q(2)	HEWM0318
	WRITE(6,125) TESTTS,TESTT2,TESTQ	HEWM0319
	GO TO 1	HEWM0320
C		HEWM0321
C	FORMAT STATEMENTS	HEWM0322
C		HEWM0323
100	FORMAT(7E8.5)	HEWM0324
101	FORMAT(84H1ANALYTICAL INVESTIGATION OF ELECTRICALLY HEATED WIRE ME	HEWM0325
	1SH FOR FLOWING GAS HEATERS, ,A6,A3,10HPROPERTIES)	HEWM0326
102	FORMAT(6HOSTAGE,I3)	HEWM0327
103	FORMAT(1H0,7X,1HD,15X,1HE,13X,4H ASF,13X,2HDE,14X,2HXL,14X,2H P,14	HEWM0328
	1X,2HAR)	HEWM0329
104	FORMAT(8E16.8)	HEWM0330
105	FORMAT(1H0,7X,2HT2,14X,2HTS,14X,2H Q,14X,2HRT)	HEWM0331
106	FORMAT (6H0INPUT)	HEWM0332
107	FORMAT(A2,I2)	HEWM0333
108	FORMAT (7H0OUTPUT)	HEWM0334
109	FORMAT(1H0,6X,2HFR,13X,3HPCE,13X,3HT11,13X,3HXL,12X,8HT2 GUESS,7X	HEWM0335
	1,8HTS GUESS,9X,7HQ GUESS)	HEWM0336
111	FORMAT(55HOTEMPERATURE EXCEEDS 5800 DEGREES RANKINE	)HEWM0337
112	FORMAT(6H0XIT =,I3)	HEWM0338
113	FORMAT(55H0ITERATIONS EXCEED 50	)HEWM0339
114	FORMAT(13H0ARGUMENT T1=,E16.8,45H EXCEEDS LIMIT OF T VS. CP CURVE	HEWM0340
	1FOR HYDROGEN)	HEWM0341
115	FORMAT(13H0ARGUMENT T1=,E16.8,45H EXCEEDS LIMIT OF T VS. CP CURVE	HEWM0342
	1FOR HELIUM )	HEWM0343
116	FORMAT(13H0ARGUMENT T1=,E16.8,45H EXCEEDS LIMIT OF T VS. CP CURVE	HEWM0344
	1FOR NITROGEN)	HEWM0345

```

117 FORMAT(13HOARGUMENT TS=,E16.8,45H EXCEEDS LIMIT OF T VS. K CURVE FHEWM0346
      1OR HYDROGEN ) HEWM0347
118 FORMAT(13HOARGUMENT TS=,E16.8,45H EXCEEDS LIMIT OF T VS. K CURVE FHEWM0348
      1OR HELIUM ) HEWM0349
119 FORMAT(13HOARGUMENT TS=,E16.8,45H EXCEEDS LIMIT OF T VS. K CURVE FHEWM0350
      1OR NITROGEN ) HEWM0351
120 FORMAT(13HOARGUMENT TS=,E16.8,45H EXCEEDS LIMIT OF T VS. MU CURVE HEWM0352
      1FOR HYDROGEN) HEWM0353
121 FORMAT(13HOARGUMENT TS=,E16.8,45H EXCEEDS LIMIT OF T VS. MU CURVE HEWM0354
      1FOR HELIUM ) HEWM0355
122 FORMAT(13HOARGUMENT TS=,E16.8,45H EXCEEDS LIMIT OF T VS. MU CURVE HEWM0356
      1FOR NITROGEN) HEWM0357
123 FORMAT(36HOPROGRAM CANNOT PROCEED TS =,E16.8) HEWM0358
124 FORMAT(8HOTS(1) =,E14.6,8H TS(2) =,E14.6,8H T2(1) =,E14.6,8H T2(2) HEWM0359
      1 =,E14.6,7H Q(1) =,E14.6,7H Q(2) =,E14.6) HEWM0360
125 FORMAT(9HOTESTTS =,E14.6,9H TESTT2 =,E14.6,8H TESTQ =,E14.6) HEWM0361
126 FORMAT(1HL) HEWM0362
      END HEWM0363
$IBFTC MGAUS MGAU0000
      SUBROUTINE MGAUSD(A,N,ANS) MGAU0001
C THIS SUBROUTINE SOLVES FROM 2-6 MGAU0002
C SIMULTANEOUS LINEAR EQUATIONS MGAU0003
      DIMENSION A(20,21),ANS(20) MGAU0004
      DOUBLE PRECISION A , ANS MGAU0005
      DO 1 I=1,N MGAU0006
1 ANS(I)=0.0D0 MGAU0007
      DO 10 I=1,N MGAU0008
        DO 9 J=I,N MGAU0009
          A(I,J+1)=A(I,J+1)/A(I,I) MGAU0010
          IF(I=N) 9,20,9 MGAU0011
6 CONTINUE MGAU0012
          K=I+1 MGAU0013
          DO 8 II=K,N MGAU0014
            DO 8 JJ=I,N MGAU0015
7 A(II,JJ+1)=-A(II,I)*A(I,JJ+1)+A(II,JJ+1) MGAU0016
10 CONTINUE MGAU0017
20 ANS(N)=A(I,J+1) MGAU0018
          IF(N=1)31,30,31 MGAU0019
30 RETURN MGAU0020
31 J=N-1 MGAU0021
          II=J MGAU0022
          DO 11 I=1,II MGAU0023
            K=J+1 MGAU0024
            DO 12 M=1,I MGAU0025
              ANS(J)=ANS(K)*A(J,K)+ANS(J) MGAU0026
12 K=K+1 MGAU0027
              ANS(J)=A(J,K)-ANS(J) MGAU0028
11 J=J-1 MGAU0029
          RETURN MGAU0030
      END MGAU0031

```

## ANALYTICAL INVESTIGATION OF ELECTRICALLY HEATED WIRE MESH FOR FLOWING GAS HEATERS, NITROGEN PROPERTIES

STAGE 1

INPUT

$C.30000000E-01$   $C.17970000E-02$   $C.55200000E-01$   $0.59400000E-02$   $0.10625000E-01$   $C.70400000E-00$   $C.42500000E-01$   
 $C.69000000E-00$   $C.10000000E-01$   $C.50000000E-03$   $0.27400000E-03$   $0.77715221E-02$   $C.34000000E-04$   $0.48352277E-02$

OUTPUT

$0.77879018E-03$   $C.33770089E-04$   $C.47809145E-02$   $0.64031472E-02$

STAGE 2

INPUT

$C.30000000E-01$   $C.17970000E-02$   $C.55200000E-01$   $0.59400000E-02$   $0.10625000E-01$   $C.70400000E-00$   $C.42500000E-01$   
 $C.69000000E-00$   $C.10000000E-01$   $C.77879018E-03$   $0.27400000E-03$   $0.10575804E-04$   $C.33770089E-04$   $C.47809145E-02$

OUTPUT

$0.10441955E-04$   $0.34997519E-04$   $C.45828684E-02$   $0.32692872E-02$

## REFERENCES

1. Siegel, Byron L.; Maag, William L.; Slaby, Jack G.; and Mattson, William F.: Heat-Transfer and Pressure Drop Correlations for Hydrogen and Nitrogen Flowing Through Tungsten Wire Mesh at Temperatures to 5200<sup>0</sup> R. NASA TN D-2924, 1965.
2. Maag, William L.; and Mattson, William F.: Forced-Convection Heat-Transfer Correlations for Gases Flowing Through Wire Matrices at Surface Temperatures to 5500<sup>0</sup> R. NASA TN D-3956, 1967.
3. Eshbach, Ovid W., ed.: Handbook of Engineering Fundamental. Second ed., John Wiley and Sons, Inc., 1952, Sec. 2-57.
4. Grier, Norman T.: Calculation of Transport Properties and Heat-Transfer Parameters of Dissociating Hydrogen. NASA TN D-1406, 1962.
5. Svehla, Roger A.: Estimated Viscosities and Thermal Conductivities of Gases at High Temperatures. NASA TR R-132, 1962.
6. Weast, Robert C., ed.: Handbook of Chemistry and Physics. 37th ed., Chemical Rubber Publishing Co., 1955, p. 2360.
7. Scarborough, James B.: Numerical Mathematical Analysis. Third ed., The Johns Hopkins Press, 1955.
8. Knudsen, James G.; and Katz, Donald L.: Fluid Dynamics and Heat Transfer. McGraw-Hill Book Co., Inc., 1958.
9. Siegel, Byron L.: Design and Operation of a High-Temperature Tungsten-Mesh Gas Heater. NASA TM X-1466, 1967.

FIRST CLASS MAIL

NOV 6 1957 51 305  
NATIONAL AERONAUTICS AND SPACE ADMINISTRATION  
FIRST CLASS MAIL

POSTMASTER: If Undeliverable (Section 158  
Postal Manual) Do Not Return

*"The aeronautical and space activities of the United States shall be conducted so as to contribute . . . to the expansion of human knowledge of phenomena in the atmosphere and space. The Administration shall provide for the widest practicable and appropriate dissemination of information concerning its activities and the results thereof."*

— NATIONAL AERONAUTICS AND SPACE ACT OF 1958

## NASA SCIENTIFIC AND TECHNICAL PUBLICATIONS

**TECHNICAL REPORTS:** Scientific and technical information considered important, complete, and a lasting contribution to existing knowledge.

**TECHNICAL NOTES:** Information less broad in scope but nevertheless of importance as a contribution to existing knowledge.

**TECHNICAL MEMORANDUMS:** Information receiving limited distribution because of preliminary data, security classification, or other reasons.

**CONTRACTOR REPORTS:** Scientific and technical information generated under a NASA contract or grant and considered an important contribution to existing knowledge.

**TECHNICAL TRANSLATIONS:** Information published in a foreign language considered to merit NASA distribution in English.

**SPECIAL PUBLICATIONS:** Information derived from or of value to NASA activities. Publications include conference proceedings, monographs, data compilations, handbooks, sourcebooks, and special bibliographies.

**TECHNOLOGY UTILIZATION PUBLICATIONS:** Information on technology used by NASA that may be of particular interest in commercial and other non-aerospace applications. Publications include Tech Briefs, Technology Utilization Reports and Notes, and Technology Surveys.

*Details on the availability of these publications may be obtained from:*

**SCIENTIFIC AND TECHNICAL INFORMATION DIVISION  
NATIONAL AERONAUTICS AND SPACE ADMINISTRATION  
Washington, D.C. 20546**